SUPPLEMENTARY INFORMATION

The microRNA miR-34a inhibits prostate cancer stem cells and metastasis by directly repressing CD44

Can Liu[1,2], Kevin Kelnar[3], Bigang Liu[1], Xin Chen[1,2], Tammy Calhoun-Davis[1], Hangwen Li[1], Lubna Patrawala[3], Hong Yan[1], Collene Jeter[1], Sofia Honorio[1], Jason Wiggins[3], Andreas G. Bader[3], Randy Fagin[4], David Brown[3] & Dean G. Tang[1,2]

[1]*Department of Molecular Carcinogenesis, the University of Texas M.D. Anderson Cancer Center, Science Park, Smithville, TX 78957, USA*

[2]*Program in Molecular Carcinogenesis, The University of Texas Graduate School of Biomedical Sciences (GSBS), Houston, TX 77030, USA*

[3]*Mirna Therapeutics, Inc., Austin, TX 78744, USA*

[4]*The Hospital at Westlake, Austin, TX 78759, USA*

This PDF contains:

Nature Medicine: doi:10.1038/nm.2284

SUPPLEMENTARY RESULTS

The expression levels of miR-34a, but not miR-34b and miR-34c, in normal prostate and prostate cancer cells correlate with the p53 status.

To determine whether miR-34a expression in normal prostate and prostate cancer cells might be regulated by p53, we employed qRT-PCR analysis to correlate the expression levels of endogenous miR-34a (localized on chromosome 1p36.22) with the p53 status in ten prostate cells (**Supplementary Fig. 1a,b**). These cells included primary prostate epithelial cell strains NHP8 (normal human prostate epithelial strain 8) and NHP9 (normal human prostate epithelial strain 9) (4); immortalized NHP9 cells (NHP9-IM) (4); cultured prostate cancer cell lines LNCaP, LNCaP C4-2 (a LNCaP subline), PC3, PPC-1, and Du145; and prostate cancer cells LAPC4 and LAPC9 freshly purified from xenograft tumors. The NHP8, NHP9, NHP9-IM, and two LNCaP lines express wild-type (wt) p53 (1,4), as evidenced by low levels of p53 protein in these cells (**Supplementary Fig. 1b**). LAPC9 cells also expressed wt p53 as revealed by our genomic DNA sequencing of exons 5-8 (data not shown). PC3 and PPC-1 cells were p53 null whereas Du145 and LAPC4 cells harbor mutant p53 (1), as supported by Western blotting analysis (**Supplementary Fig. 1b**). qRT-PCR analysis revealed that the four prostate cancer cells harboring mutant or null p53 displayed much lower levels of miR-34a than the six cell types with wt p53 (**Supplementary Fig. 1a**; note that we utilized PPC-1 cells, which expressed the lowest level of miR-34a mRNA, as the normalization control), suggesting that p53 regulates the baseline miR-34a expression in prostate and prostate cancer cells. Interestingly, among the six p53-wt cells, LNCaP and C4-2 cells expressed higher levels of miR-34a than NHP8, NHP9, NHP9-IM, and LAPC9 cells (**Supplementary Fig. 1a**).

To determine whether p53 may also regulate the baseline expression levels of the other two miR-34 family members, miR-34b and miR-34c, which are localized on chromosome 11 q23.1 and were not differentially expressed between the $CD44^+$ and $CD44^-$ prostate cancer cells, we also employed qRT-PCR to measure their levels in the same ten prostate cells. In contrast to miR-34a, miR-34a and miR-34c showed similar expression patterns and were not strictly correlated with the p53 status (**Supplementary Fig. 1a**). For

Nature Medicine: doi:10.1038/nm.2284

example, in p53 null or mutant cells, although PPC-1, PC3, and LAPC4 cells exhibited undetectable miR-34b and miR-34c, Du145 cells showed extremely high levels of both miRNAs (**Supplementary Fig. 1a**), suggesting p53-independent regulation of miR-34b and miR-34c in certain prostate cancer cells. Similarly, miR-34b and miR-34c levels showed wide variations in the six p53-wt cells.

Finally, we measured the baseline levels of let-7b in the ten prostate cells as this miRNA was also downregulated in the $CD44^+$ prostate cancer cells (**Fig. 1b**). The let-7b expression pattern was somewhat like that of miR-34a in that it was much higher in LNCaP and C4-2 cells (**Supplementary Fig. 1a**). However, unlike miR-34a, its expression was readily detectable in p53 mutant or null prostate cancer cells (**Supplementary Fig. 1a**).

Transfection of miR-34a oligos induced cell-cycle arrest, apoptosis or senescence in p53-mutant and p53-null prostate cancer cells.

Since p53 is frequently mutated in advanced prostate cancer, we transfected p53-mutant or null Du145, PC3, and PPC-1 cells with synthetic mature miR-34a oligonucleotides (oligos) or the negative control miRNA (miR-NC or NC) that contains a scrambled sequence and does not specifically target any human gene products (**Supplementary Fig. 1c**). The miR-34a mimics the dicer cleavage product that is loaded into the RISC in the cytoplasm and therefore, no processing of the pre-miRNA is required for it to be activated (thus it represents a mature miRNA). Transfected miR-34a oligos caused inhibitory effects in all three prostate cancer cells (**Supplementary Figs. 2** and **3**). In Du145 cells, miR-34a oligo transfection reduced cell numbers and population doublings (**Supplementary Fig. 2a,b**) as a result of inhibition of cell proliferation (**Supplementary Fig. 2c**). In PC3 cells, miR-34a oligos inhibited population doublings by causing apoptosis (**Supplementary Fig. 3a–c**). In PPC-1 cells, transfected miR-34a oligos inhibited proliferation, increased senescence, and induced apoptosis resulting in reduced total cell numbers and cumulative population doublings (**Supplementary Fig. 3d–g**).

Nature Medicine: doi:10.1038/nm.2284

SUPPLEMENTARY METHODS

Cells and animals. We obtained prostate cancer cell lines, LNCaP, LNCaP C4-2, PC3, PPC-1, and Du145, from ATCC and maintained them as described[1-3]. Primary and immortalized normal human prostate (NHP) epithelial cells were detailed elsewhere[4]. We purified LAPC4 and LAPC9 (and, sometimes, Du145) cells from xenograft tumors (see below)[3,5-8]. Immune-deficient mice, NOD–SCID (non-obese diabetic severe combined immune deficient) and NOD–SCIDγ, were produced mostly from our own breeding colonies and purchased occasionally from the Jackson Laboratories (Bar Harbor) and maintained in standard conditions according to the Institutional guidelines. All animal experiments were approved by our institutional IACCUC.

Prostate cancer cell purification. We routinely maintained human xenograft prostate tumors, *i.e.*, LAPC9 (bone metastasis; AR^+ and PSA^+), LAPC4 (lymph node metastasis; AR^+ and PSA^+), and Du145 (brain metastasis; AR^- and PSA^-), in NOD–SCID mice. We first purified human prostate cancer cells out of xenografts by depleting murine cells. $CD44^+$ and $CD44^-$ cells were further purified using fluorescence-activated cell sorting (FACS) with the purities of both populations being >98% (5,6). $CD133^+$ and $CD133^-$ LAPC4 cells were purified using biotinylated monoclonal antibody to CD133 (AC133) and the magnetic beads (MACS) by following the manufacturer's instructions (Miltenyi Biotech). Post-sort analysis revealed purities of both populations being >95%. We purified the side population (SP) of LAPC9 cells by FACS as previously described[3]. We obtained primary human prostate tumors (HPCa; Supplementary Table 1) with the patients' consent from Da Vinci robotic surgery. All work with HPCa samples was approved by the M.D. Anderson Cancer Center Institutional Review Board (IRB LAB04-0498). We purified epithelial HPCa cells through a multi-step process and by depleting lineage-positive hematopoietic, stromal, and endothelial cells[4,7,8]. We then purified Lin^-CD44^+ HPCa cells using MACS or FACS (Supplementary Table 1).

Transient transfection with oligos. We plated bulk or purified $CD44^+$ prostate cancer cells 24 h before transfection with 33 nM of miR-34a or non-targeting negative control miRNA (miR-NC) oligos (Ambion) by using Lipofectamine 2000 (Invitrogen). Alternatively, we transfected bulk or purified $CD44^-$ prostate cancer cells with 33 nM of anti-miR-34a (anti-34a) or anti-miR-NC (anti-NC) oligos (Ambion). In some experiments (see below), oligos were electroporated into prostate cancer cells. We generally harvested the transfected cells for *in vitro* or *in vivo* studies after culturing for overnight to 24 h.

Retroviral and lentiviral mediated overexpression of miR-34a. Basic retroviral and lentiviral procedures were previously described[4,7] and the key vectors used in the present study were presented in Supplementary Fig. 1d. An MSCV retroviral vector directing the expression of pre-miR-34a (MSCV-34a) and the empty control vector, MSCV-PIG (Puromycin-IRES-GFP), were used in previous studies[9]. prostate cancer cells were infected with the retroviral supernatant for 48 h in the presence of 8 μg ml^{-1} polybrene. Two days after infection, puromycin was added to the media at 3 μg ml^{-1}, and cell populations were selected for 2 weeks. A lentiviral vector encoding pre-miR-34a (lenti-34a) and the control vector

Nature Medicine: doi:10.1038/nm.2284

(lenti-ctl) (Supplementary Fig. 1d) were obtained from Systems Biosciences (SBI). Lentivirus was produced in 293FT packaging cells and titers determined for GFP using HT1080 cells. prostate cancer cells were infected at an MOI of 10 - 20 and harvested 48–72 h post-infection.

Experiments correlating miR-34a levels in normal prostate and prostate cancer cells with the p53 status. We employed qRT-PCR to quantify the levels of miR-34a, and, for comparisons, of miR-34b, miR-34c, and let-7b in NHP8, NHP9, and NHP9-IM, LNCaP, LNCaP C4-2, PC3, PPC-1, Du145, LAPC4, and LAPC9 cells. For qRT-PCR analysis[10], we prepared total RNA from these cells and assayed the levels of miR-34a (assay ID 000426, TaqMan miRNA Assay, ABI), miR-34b (ABI assay ID 000427), miR-34c (ABI assay ID 000428), and hsa-let-7b (let-7b; ABI assay ID 000378).

BrdU incorporation assays, senescence β-gal (SA-βgal) staining, Western blotting, immunofluorescence, flow cytometry analysis (FACS), and immunohistochemistry (IHC). These procedures were previously described[2-8]. For Western blotting of p53 in ten prostate cells, protein lysate (50 μg) was separated on SDS-PAGE, transferred to nitrocellulose membrane, and probed with a monoclonal Ab to p53 (clone MO-1). For characterization of the knockdown effect of pGIPz-CD44shRNA, PC3 or Du145 cells were infected with this vector or the pGIPz control vector (MOI 20; 72 h) and cells were harvested for Western blotting of CD44 or β-actin (loading control) (see Supplementary Fig. 1d).

***In vitro* effects of miR-34a overexpression on bulk prostate cancer cells.** For studies in Du145 cells, we first electroporated cells (Bio-Rad GenePulserXcell, 150 mV, 25 mS) in 200 μl of serum-free OPTIMEM in triplicate with 1.6 μmol L^{-1} miR-34a or miR-NC oligos. Immediately after electroporation, we added 800 μl of serum-containing medium to each cuvette, and plated one million live cells in triplicate on d 0. At the end of 1 week, cells were dissociated, counted, re-electroporated (600,000 cells/well in triplicate), and plated. We repeated this process one week later at d 14 and terminated the whole experiment at the end of the third week (d 21). We then determined the cumulative cell numbers and population doublings (PDs). For BrdU incorporation assays, we transfected Du145 cells with miR-NC or miR-34a oligos (33 nM) using Lipofectamine and plated cells at two different densities (*i.e.*, 10,000 or 5,000 cells/well) on glass coverslips. Cells were terminated either 2 or 5 d after plating and used in BrdU staining.

For studies in PC3 cells, we also electroporated cells with miR-NC or miR-34a oligos, plated one million cells of each type in triplicate, and cultured them in RPMI-1640 plus 7% FBS. At the end of one week, cells were photographed and then dissociated, counted, re-electroporated (600,000 cells each in triplicate), and replated. The procedure was repeated at the end of the second week and at the end of the third week (*i.e.*, 21 d), cells were harvested and experiments terminated. We electroporated PPC-1 cells with miR-NC or miR-34a oligos on d 0 and carried out subsequent experiments as for PC3 cells except that we enumerated cells every 2–3 d. For BrdU assays, we transfected PPC-1 cells with miR-NC or miR-34a oligos (33 nM) for 24 h and then plated 15,000 cells each on glass coverslips. 24 h later, we terminated cells and performed BrdU staining.

Nature Medicine: doi:10.1038/nm.2284

Clonal, clonogenic, and sphere-formation assays. *For holoclone assays*[8,11], we plated prostate cancer cells at a clonal density (*i.e.*, 100 cells/well) in a 6-well dish, counted the number of holoclones several days later, and presented the percentage of cells that established a holoclone as cloning efficiency. *For clonogenic assays*[5,7,8], we plated cells generally at 1,000 cells/well in Matrigel (MG) or methylcellulose (MC) at 1:1 ratio in 100–200 μl and enumerated colonies 1–2 weeks after plating. *For sphere-formation assays*[5,7,8], we generally plated cells at 5,000–10,000 cells/well in serum-free prostate epithelial basal medium (PrEBM) supplemented with 4 μg ml^{-1} insulin, B27 (Invitrogen), and 20 ng ml^{-1} EGF and bFGF in ultra-low attachment (ULA) plates. Floating spheres that arose in 1–2 weeks were counted. For sphere-formation assays in HPCa cells, we purified HPCa cells from human primary tumors, i.e., HPCa101 (Gleason 9), HPCa107 (Gleason 7), HPCa109 (Gleason 7), and HPCa112 (Gleason 6), and infected with lenti-ctl or lenti-34a vectors (MOI 20) overnight. Next day, equal numbers of live cells (20,000/well) were plated in triplicate in ULA plates in serum-free medium containing B27, EGF, and bFGF and spheres enumerated at 11 d (for HPCa107), 33 d (for HPCa109), or 9 d (for HPCa112) after plating. For all above experiments, we run a minimum of triplicate wells for each condition and repeated experiments whenever feasible.

Tumor transplantation experiments. Basic procedures for subcutaneous (s.c) and orthotopic (DP) tumor transplantations can be found in our earlier publications[3-8]. *For tumor experiments in LAPC9 cells*, we acutely purified LAPC9 cells from the maintenance tumors and transfected with miR-34a or miR-NC oligos (33 nM). 24 h later, 100,000 cells each were implanted, in 50% Matrigel, into the DP of intact male NOD-SCID mice. *For tumor experiments in LAPC4 cells*, we freshly purified LAPC4 cells from xenograft tumors and transfected with miR-NC or miR-34a oligos (33 nM). 100,000 cells each were injected s.c in male NOD-SCID mice. Alternatively, purified LAPC4 cells were infected with either the control (lenti-ctl) or lenti-miR-34a (lenti-34a) lentiviral vectors (both at an MOI of 10). 24 h after infection, 10,000 cells each were injected s.c in male NOD-SCID mice. *For tumor experiments in Du145 cells*, in addition to oligo transfection, we also infected cultured Du145 cells with either the control retroviral vector (MSCV-PIG) or a retroviral vector encoding miR-34a (MSCV-34a)(9), followed by puromycin selection and s.c injection in Matrigel. Alternatively, Du145 cells were infected with lenti-ctl or lenti-34a vectors (MOI 10) and, 24 h after infection, 10,000 cells of each type (n = 10) were injected s.c in NOD-SCID mice. *For tumor experiments in PPC1 cells*, we electroporated cultured PPC-1 cells with miR-34a or NC oligos (1.6 μM or 5 μg) on d 0. We injected 500,000 live cells s.c in NOD-SCID mice and measured tumor volumes, using a digital caliper, starting from d 3. On d 7, 13, 20, and 25, we injected miR-NC or miR-34a oligos mixed with siPORT amine (Ambion) intra-tumorally[10].

Experiments with HPCa58 early-generation xenograft tumors. HPCa58 xenograft tumor

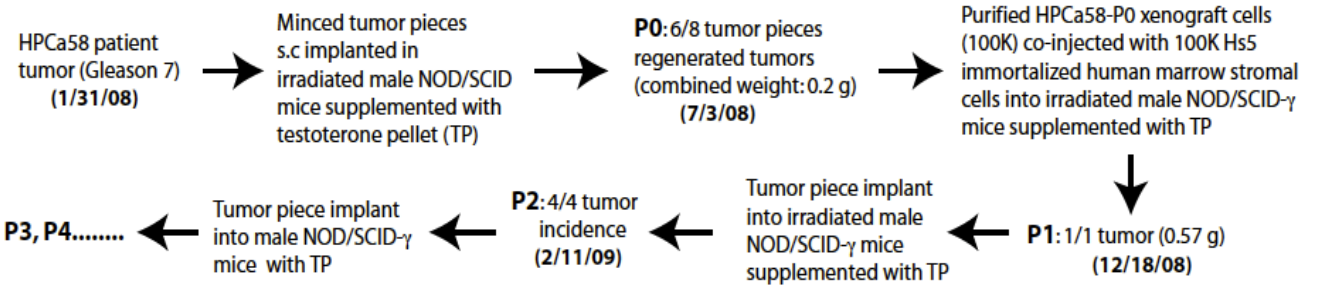

Nature Medicine: doi:10.1038/nm.2284

was established using the *Scheme* below. Briefly, the primary tumor pieces were first implanted into γ-irradiated (4 Gy; X-ray) male NOD-SCID mice. The P0 xenograft tumors were pooled and used to purify out human prostate cancer cells as described above, which were then co-injected with the Hs5 immortalized human marrow stromal cells in male NOD-SCIDγ mice. Subsequent passaging of the first-generation (P1) xenografts was performed by implanting tumor pieces or by injecting purified HPCa58 cells alone without Hs5 cells. We have utilized similar strategies to establish about 8 early-generation human prostate cancer xenografts (including HPCa87 and HPCa91 xenografts; see Supplementary Table 1). These xenograft tumors were of the human origin and morphologically epithelial with detectable cytokeratin 8 and 18. RT-PCR analysis detected *AR* whereas Western blotting detected racemase expression in most xenografts (Chen et al., manuscript in preparation). For the present study, HPCa58 cells were purified from a P3 xenograft tumor (see *Scheme*) and infected with lenti-ctl or lenti-34a vectors (MOI 20). 24 h later, 100,000 cells of each were s.c injected into the NOD-SCIDγ mice. The 1° tumors were harvested 21 d later and 10,000 purified GFP^+ (*i.e.*, infected) tumor cells from respective 1° tumors were injected and the 2° tumors were harvested 26 d later.

Monitoring metastasis. For metastasis analysis[5,8], we first observed tumor-bearing animals for symptoms such as hunched posture, irregular breathing and gait, and paraplegia. When systemic symptoms or primary tumor burden became obvious or when the animals became moribund, we sacrificed them by CO2 euthanization and cervical dislocation. We then performed comprehensive necropsy to isolate individual organs, which were examined for gross metastases. Finally, GFP^+ metastatic foci in each organ (primarily, the lung) were examined and quantified under a Nikon SMZ1500 whole-mount epifluorescence dissecting microscope.

Measuring cell migration by time-lapse videomicrocopy

We seeded bulk Du145 or purified $CD44^+$ and $CD44^-$ cells onto the glass-bottom dish (CELLview^{tm}, 4 compartments, Greiner Bio-One GmbH) and cultured them overnight to create a monolayer. We introduced a homogeneous ‘wound’ track using the tip of a fine forceps. Cells were washed with PBS to remove the debris and smoothen the wound edges. We then placed cells in the culture chamber connected to the time-lapse microscope (Nikon, BioStation IM). We acquired phase-contrast images of at least 20 selected fields of each group at the interval of 30 min for a total of 24 h. We analyzed images using the NIS Elements software (Nikon, NIS elements- 2.35) and quantified cell migration by measuring the time required to close the induced wounds.

Statistical analyses. In general, we used unpaired two-tailed Student’s *t*-test to compare differences in cell numbers, cumulative PDs, percentages of $CD44^+$, % $BrdU^+$ or SA-βgal^+ cells, cloning efficiency, tumor weights, migration, invasion, and other related parameters. We employed Fisher’s Exact Test and χ^2 test to compare incidence and latency. We used the Log-Rank test to analyze the survival curves and ANOVA (F-test) to compare differences in multiple groups. In all these analyses, a $P < 0.05$ was considered statistically significant.

Nature Medicine: doi:10.1038/nm.2284

SUPPLEMENTARY REFERENCES

1. Pienta, K.J. *et al*. The current state of preclinical prostate cancer animal models. *Prostate* **68**, 629-639 (2008).
2. Bhatia, B. *et al*. Evidence that senescent human prostate epithelial cells enhance tumorigenicity: Cell fusion as a potential mechanism and inhibition by p16INK4a and hTERT. *Int. J. Cancer* **122**, 1483-1495 (2008).
3. Patrawala, L. *et al*. Side population (SP) is enriched in tumorigenic, stem-like cancer cells whereas ABCG2$^+$ and ABCG2$^-$ cancer cells are similarly tumorigenic. *Cancer Res*. **65**, 6207-6219 (2005).
4. Bhatia, B. *et al*. Critical and distinct roles of p16 and telomerase in regulating the proliferative lifespan of normal human prostate epithelial progenitor cells. *J. Biol. Chem.* **283**, 27957-27972 (2008).
5. Patrawala, L. *et al*. Highly purified CD44$^+$ prostate cancer cells from xenograft human tumors are enriched in tumorigenic and metastatic progenitor cells. *Oncogene* **25**, 1696-1708 (2006).
6. Patrawala, L., Calhoun-Davis, T., Schneider-Broussard, R. & Tang, D.G. Hierarchical organization of prostate cancer cells in xenograft tumors: the CD44$^+\alpha 2\beta 1^+$ cell population is enriched in tumor-initiating cells. *Cancer Res.* **67**, 6796-6805 (2007).
7. Jeter, C. *et al*. Functional evidence that the self-renewal gene NANOG regulates human tumor development. *Stem Cells* **27**, 993-1005, 2009.
8. Li, H.W. *et al*. Methodologies in assaying prostate cancer stem cells. *Methods Mol. Biol.* **569**, 85-138 (2009).
9. He, L. *et al*. A microRNA component of the p53 tumour suppressor network. *Nature* **447**, 1130-1134 (2007).
10. Wiggins, J.F. *et al*. Development of a lung cancer therapeutic based on the tumor suppressor microRNA-34. *Cancer Res*. 70, 5923-5930 (2010).
11. Li, H.W., Chen, X., Calhoun-Davis, T., Claypool, K. & Tang, D.G. PC3 Human prostate carcinoma cell holoclones contain self-renewing tumor-initiating cells. *Cancer Res*. 68, 1820-1825 (2008).

Nature Medicine: doi:10.1038/nm.2284

Supplementary Figure 1. miR-34a levels in prostate cells correlate with p53 status.

(a) qRT-PCR quantification of miR-34a, miR-34b, miR-34c, and let-7b in 10 prostate cell lines. The relative expression levels (mean ± S.D) are presented by setting the miRNA levels in PPC-1 cells as one. Shown below the bar graphs are the p53 statuses (N, null; M, mutant; W, wild-type) and the % of $CD44^+$ cells in each cell type as determined by flow cytometry or immunofluorescence staining (U.D, undetectable).

(b) Western blotting of p53 in prostate (cancer) cells.

(c) The four oligonucleotides (oligos) used in the current study. All oligos were obtained from Ambion and at least 3 studies (references indicated) have utilized and characterized miR-34a and miR-NC oligos. Use of anti-miR-NC oligos has been published in at least one study (i.e., reference 25) and anti-miR-34a was characterized in the present study.

(d) Retroviral and lentiviral vectors utilized in the present study. Shown at the bottom was the characterization of the knockdown effect of pGIPz-CD44shRNA by Western blotting.

Nature Medicine: doi:10.1038/nm.2284

Supplementary Figure 1

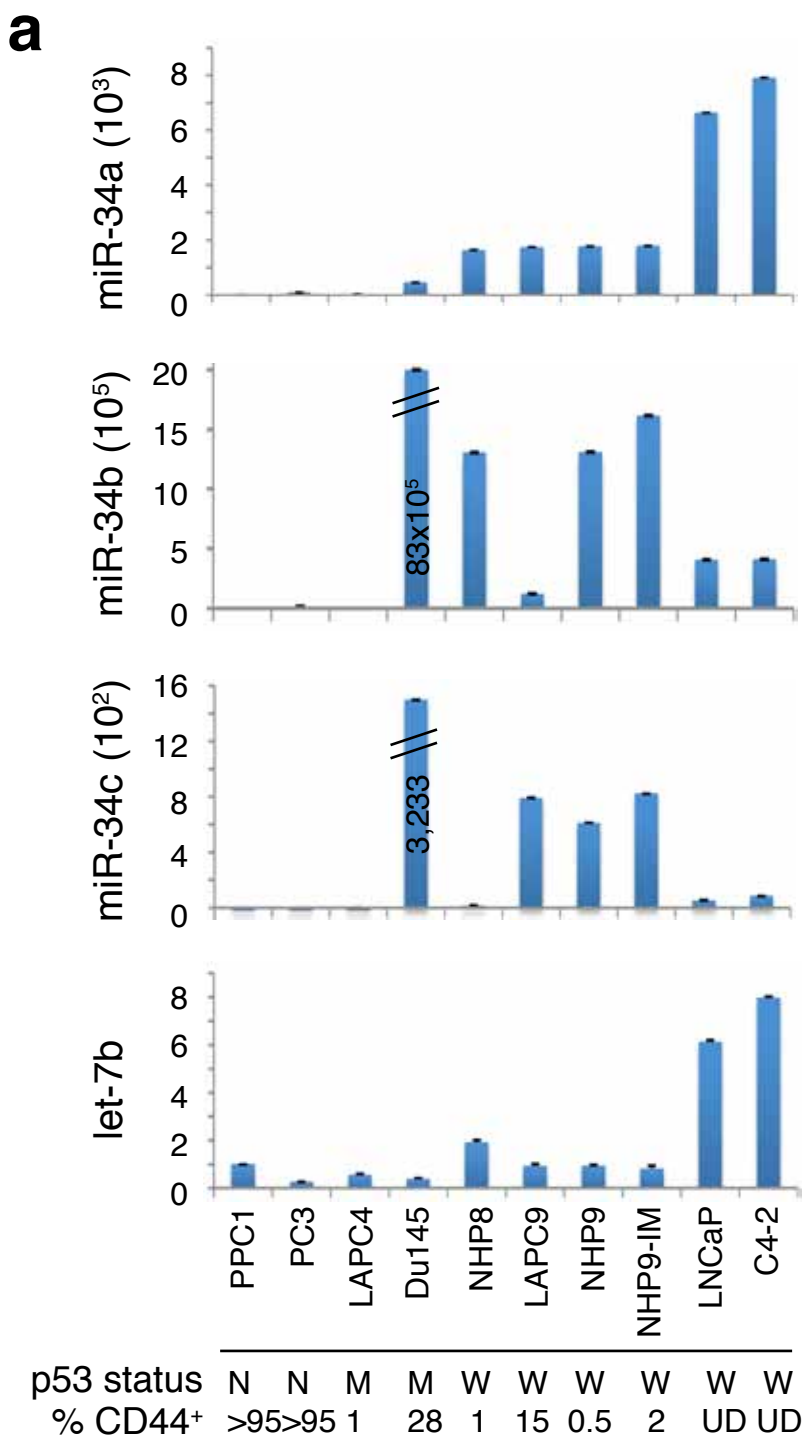

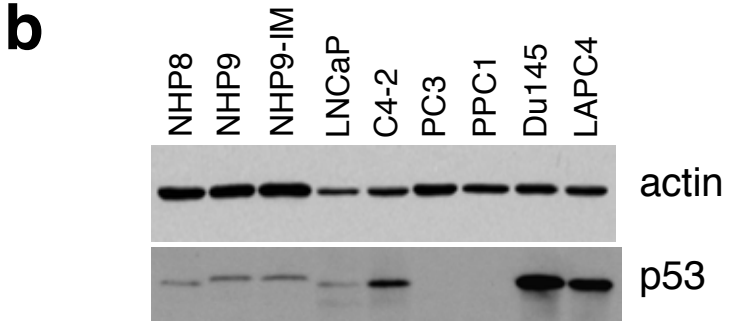

c

Name	Source	Ref.
miR-34a (mature) oligos	Ambion	26,31,32
miR-NC (neg. control) oligos	Ambion	26,31,32
anti-miR-34a oligos	Ambion	this study
anti-miR-NC oligos	Ambion	25

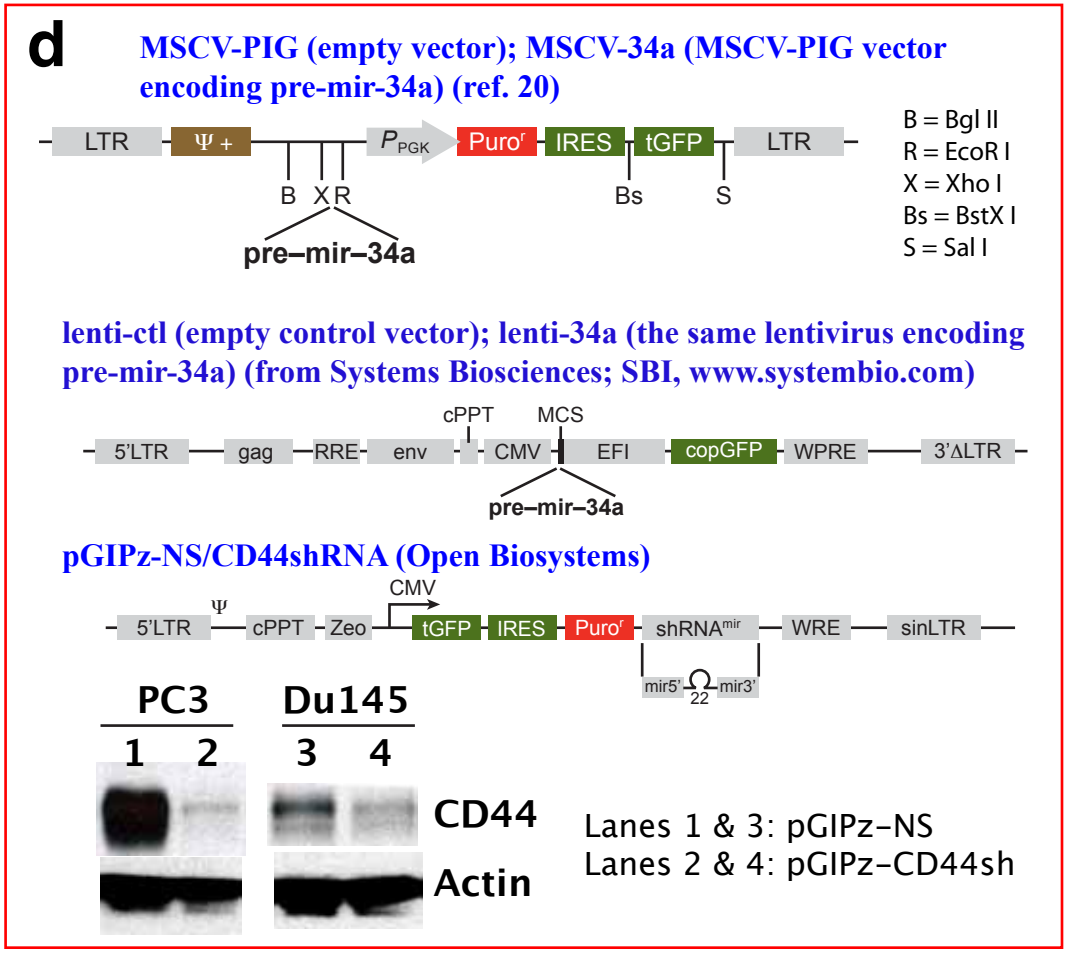

Nature Medicine: doi:10.1038/nm.2284

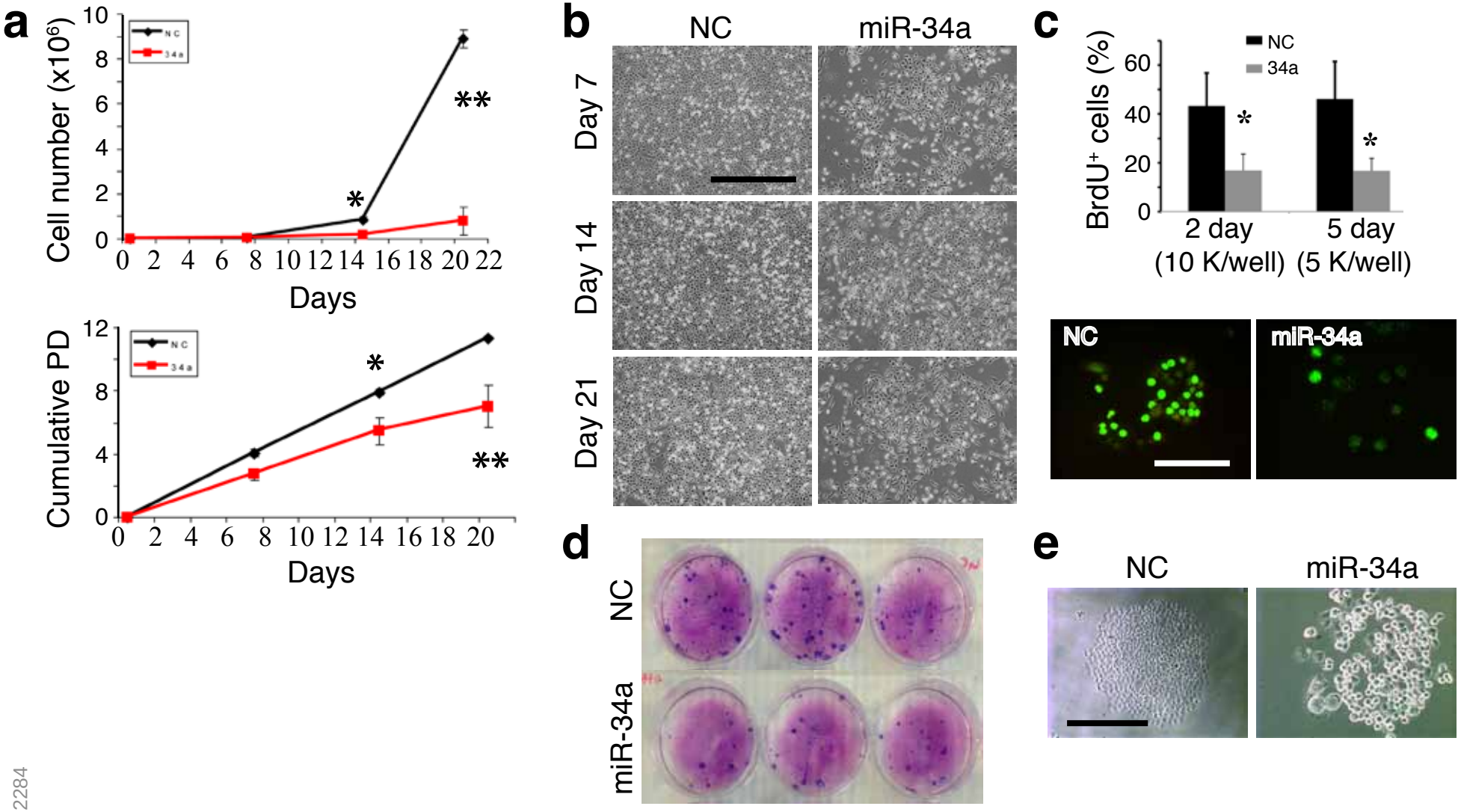

Supplementary Figure 2. miR-34a inhibits Du145 cell proliferation and clonal expansion.

(**a**,**b**) Exogenous miR-34a reduces Du145 cell number. Plotted is the cumulative cell numbers or population doublings (PDs) as a function of time and bars represent the mean ± S.D (*$P < 0.05$; **$P < 0.001$). Shown in b are representative microphotographs (scale bar, 10 μm). (**c**) miR-34a inhibits Du145 cell proliferation. Presented is the mean % of BrdU-positive cells counted from a total of 800–1,000 cells performed under two conditions (*$P < 0.001$). Below are representative images (scale bar, 10 μm) of BrdU staining in the 2-d samples. (**d,e**) miR-34a inhibits Du145 clonal expansion. Cells transfected with miR-NC or miR-34a oligos (33 nM) were plated in triplicate at 100 cells/well. The experiment was terminated at 9 d and wells were Giemsa-stained (d). Shown in e are clonal images (scale bar, 10 μm). Results shown in d and e were representative of two independent experiments.

Nature Medicine: doi:10.1038/nm.2284

Supplementary Figure 3. Effects of miR-34a overexpression on PC3 and PPC-1 cells.

(**a**,**b**) Exogenous miR-34a reduces PC3 cell number. Cumulative cell numbers and PDs were presented and bars represent the mean ± S.D (*$P < 0.05$; **$P < 0.001$). Shown in b are representative microphotographs of treated PC3 cells at 7, 14, and 21 d post treatment (scale bar, 10 μm).

(**c**) miR-34a induces apoptosis in PC3 cells. Samples harvested at the end of 21 d (above) were used in DEVDase assays, which measure caspase-3 or 7 (C3/7) activities.

(**d**,**e**) miR-34a transfection reduces PPC-1 cell number. PPC-1 cells were electroporated with miR-NC or miR-34a oligos on d 0 and subsequent experiments were carried out as for PC3 cells except that cells were enumerated every 2-3 d using triplicate samples and re-electroporation was done on d 4 and 11, respectively (arrows). Cumulative cell numbers and PDs were presented (d). Shown in e are representative microphotographs (scale bar, 10 μm) of treated PPC-1 cells at d 7.

(**f**–**i**) miR-34a inhibits PPC-1 cell proliferation and induces senescence. Presented in f is the % of $BrdU^+$ cells (mean ± S.D; $n = 3$). g, 100,000 PPC-1 cells transfected with NC or miR-34a oligos were plated for SA-βgal staining. Shown are total number of SA-βgal^+ cells in each well ($n = 3$) and representative microphotographs (below; scale bar, 10 μm). h, Holoclone assays in PPC-1 cells. 500 cells/well were plated in triplicate and holoclones imaged on d 5 (scale bar, 25 μm). i, Sphere-formation assays. 1,000 PPC-1 cells transfected with miR-NC or miR-34a oligos were plated in triplicate in 6-well ULA plates. Spheres were counted on d 10. Bars are mean ± SD ($n = 3$).

Nature Medicine: doi:10.1038/nm.2284

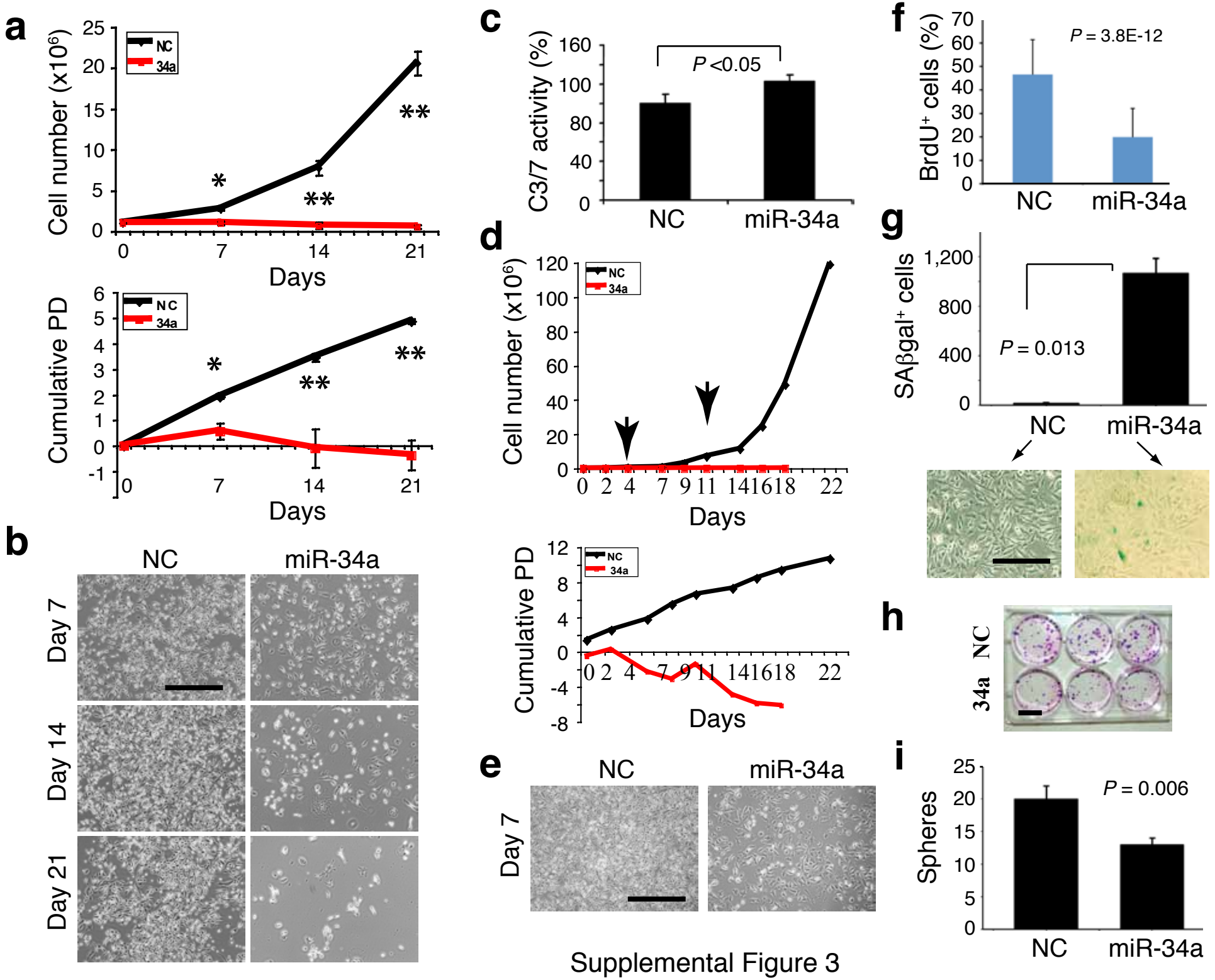

Supplemental Figure 3

Nature Medicine: doi:10.1038/nm.2284

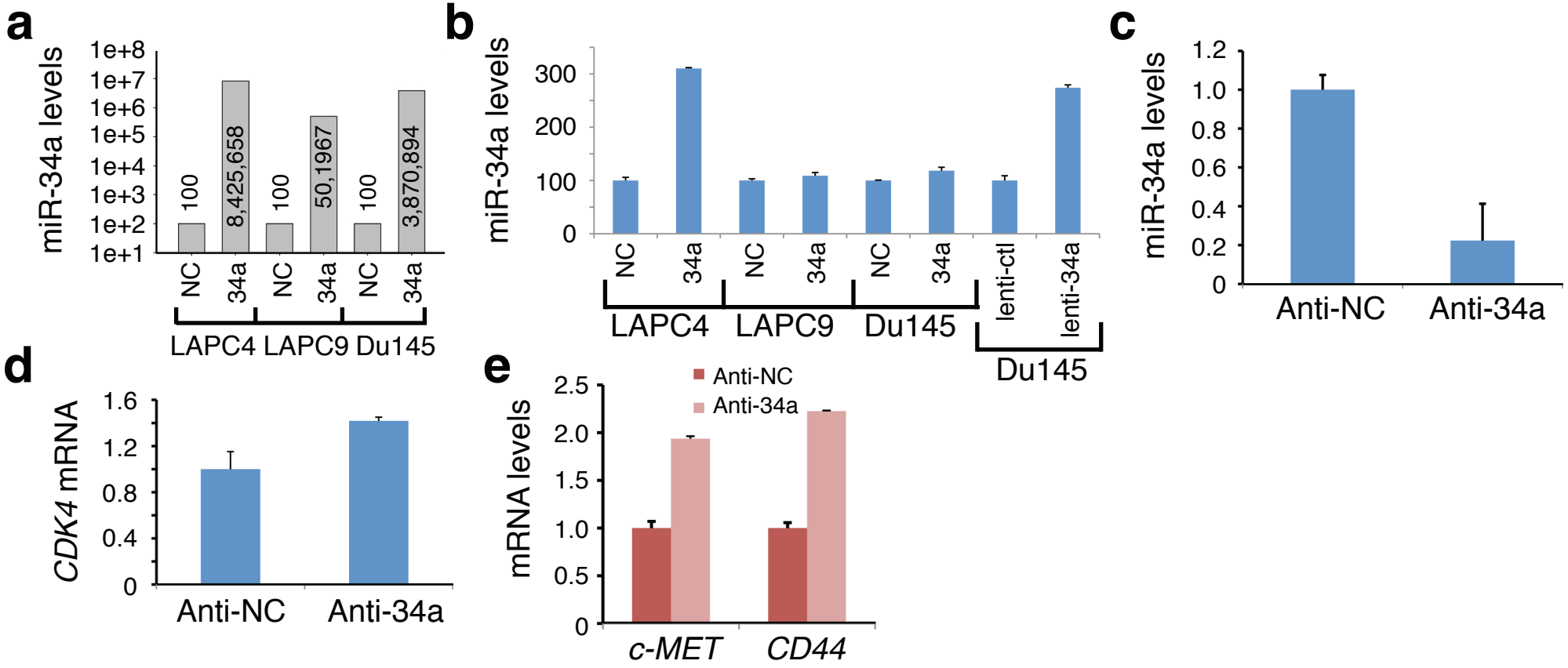

Supplementary Figure 4. Validations of miR-34a and anti-miR-34a.

(**a**) PCa cells freshly transfected with miR-34a oligos showed miR-34a levels several orders of magnitude higher than those transfected with miR-NC oligos. The indicated PCa cells purified from xenograft tumors were transfected with miR-34a or miR-NC oligos and, 24 h later, were harvested and used in tumor experiments whereas a small number of cells were set aside and used in qRT-PCR measurement of miR-34a. Shown are the mean miR-34a levels (in log scale; $n = 3$) in miR-34a transfected cells relative to those in the miR-NC transfected cells (actual mean values indicated in the bars).

(**b**) Loss of miR-34a in residual tumors. Residual tumors (see Supplementary Fig. 5) derived from cells transfected with miR-34a oligos or from Du145 cells infected with lenti-34a were used in qRT-PCR analysis of miR-34a. Shown are the miR-34a levels (in linear scale; mean ± S.D) relative to the respective control tumors.

(**c**) Anti-miR-34a reduces endogenous miR-34a levels. LAPC9 cells were transfected with anti-NC or anti-34a oligos (33 nM) and harvested 24 h later to prepare total RNA for qRT-PCR analysis of miR-34a. Presented are the relative levels normalized to the control miR-191 and miR-24 with the miR-34a in anti-NC-transfected cells set at one.

(**d**) Anti-miR-34a increases the *CDK4* mRNA levels. LAPC9 cells prepared as above were used in qRT-PCR measurement of *CDK4* mRNA (see Supplementary ref. 10). The abundance of *CDK4* mRNA was expressed as the levels relative to the anti-NC transfected cells.

(**e**) Anti-miR-34a increases the mRNA levels of c-MET and CD44. Du145 tumors from $CD44^-$ cells transfected with anti-34a or anti-NC were used in qRT-PCR of *c-MET* and *CD44* mRNAs (mean ± S.D; $n = 3$).

Nature Medicine: doi:10.1038/nm.2284

Supplementary Figure 5. Effects of miR-34a on tumor growth

Indicated are tumor incidence (tumors developed/numbers of injections; %), harvest time (including actual injection and termination dates), mean tumor weight (in grams), and the *P* values for tumor weights. Gross tumor images are not to the same scale.

(**a**) miR-34a oligo transfection inhibits orthotopic LAPC9 tumor regeneration.

(**b**) miR-34a oligo transfection inhibits LAPC4 tumor growth.

(**c**) miR-34a overexpression by lentiviral infection inhibits LAPC4 tumor growth. Note that all lenti-ctl tumors were green whereas most lenti-34a tumors were white and had little GFP-positive cells, suggesting that the small lenti-34a tumors were derived from the uninfected cells or from the infected cells that had lost miR-34a expression.

(**d**) miR-34a oligo transfection inhibits Du145 tumor growth.

(**e**) miR-34a overexpression by retroviral infection inhibits Du145 tumor regeneration. The MSCV-34a tumors were ~3 times smaller than the control tumors but the difference was at the statistical borderline due to small numbers of animals in each group that developed tumors.

(**f**) miR-34a overexpression by lentiviral infection inhibits Du145 tumor growth. Tumors were harvested at 49 d.

(**g**) miR-34a inhibits PPC-1 tumor development. Animals were terminated on d 46. Arrowheads indicate repeated intra-tumoral oligo injections. Shown are the tumor volumes (mean ± S.D; $n = 7$ for each group) measured on the indicated time points (d).

(**h**) miR-34a re-expression in purified $CD44^+$ LAPC9 inhibits tumor regeneration.

(**i**) Anti-miR-34a promotes tumor growth of purified $CD44^-$ Du145 cells. This represents an independent repeat experiment to Fig. 1h.

Nature Medicine: doi:10.1038/nm.2284

a

LAPC9 (100,000 cells/DP inj.)	Incidence	Harvest	Weight (g)	P value
miR-NC	8/8 (100%)	38 d (2/21/08 - 3/31/08)	0.62 ± 0.44	
miR-34a	5/7 (71%)	38 d	0.28 ± 0.15	0.038

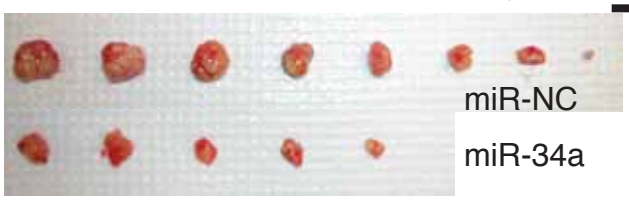

b

LAPC4 (100,000 cells/s.c inj.)	Incidence	Harvest	Weight (g)	P value
miR-NC	8/8 (100%)	10 d (2/03/08 - 2/13/08)	0.56 ± 0.27	
miR-34a	6/8 (75%)	10 d	0.29 ± 0.16	0.02

c

LAPC4 (10,000 cells/s.c inj.)	Incidence	Harvest	Weight (g)	P value
lenti-ctl	6/6 (100%)	69 d (2/11/09 - 4/21/09)	0.54 ± 0.32	
lenti-34a	6/6 (100%)	69 d	0.15 ± 0.09	0.015

d

Du145 (100,000 cells/s.c inj.)	Incidence	Harvest	Weight (g)	P value
miR-NC	8/8 (100%)	62 d (1/31/09 - 4/03/09)	0.82 ± 0.39	
miR-34a	8/8 (100%)	62 d	0.5 ± 0.18	0.03

e

Du145 (100,000 cells/s.c inj.)	Incidence	Harvest	Weight (g)	P value
MSCV -PIG	5/10 (50%)	37 d (1/29/09 - 3/07/09)	0.71 ± 0.47	
MSCV -34a	2/10 (20%)	37 d	0.28 ± 0.15	0.05

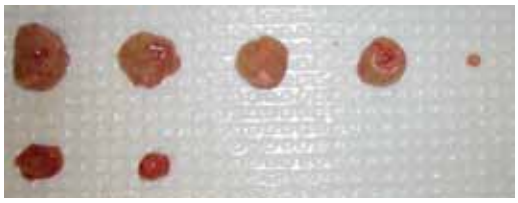

f

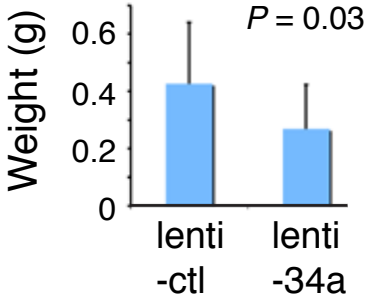

g

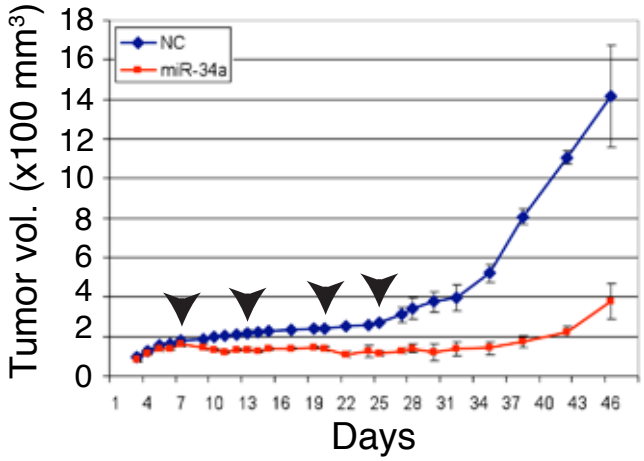

h

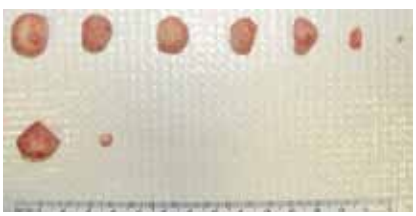

CD44+ LAPC9 cells (10K/inj; 43 d)

i

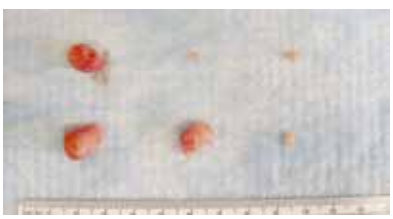

CD44- Du145 cells (10K/inj; 82 d)

Supplementary Figure 5

Nature Medicine: doi:10.1038/nm.2284

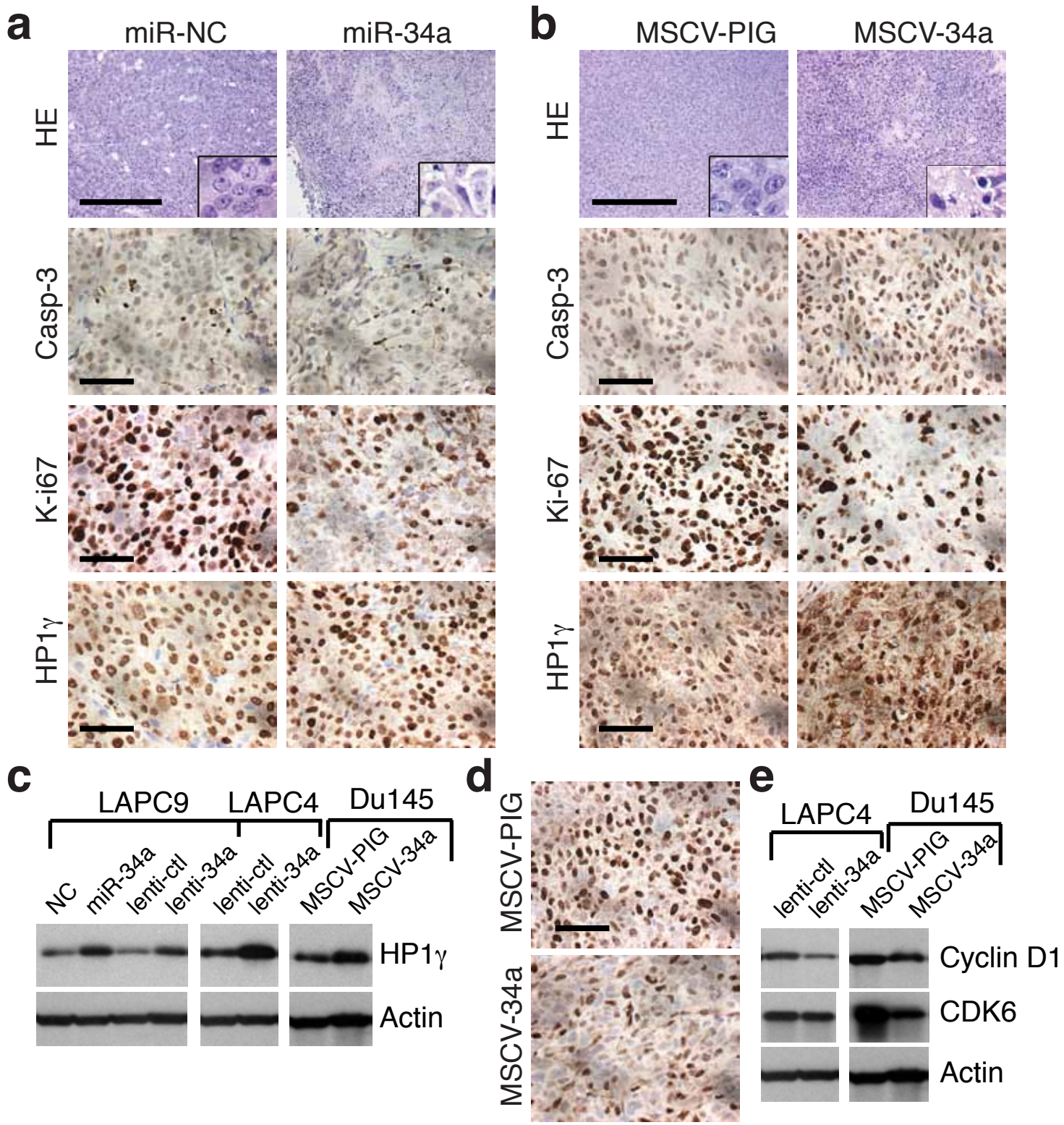

Supplementary Figure 6. Characterizations of miR-34a-overexpressing tumors.

(**a**,**b**) Paraffin-embedded sections of LAPC9 tumors (a) derived from cells transfected with miR-NC or miR-34a oligos (Supplementary Fig. 5a) or Du145 tumors (b) derived from cells infected with MSCV-PIG or MSCV-34a (Supplementary Fig. 5e) were used in HE or IHC staining for the molecules indicated. Depicted in the insets in the top rows is a more differentiated morphology of the cells in miR-34a overexpressing tumors. Shown below are representative images displaying reduced Ki-67 and increased HP1γ but no changes in active caspase-3 in the miR-34a overexpressing tumors. Scale bars, 20 μm.

(**c**) Increased HP-1γ in tumors derived from PCa cells overexpressing miR-34a by Western analysis.

(**d**,**e**) IHC (d) and Western blotting (e) showing reduced cyclin D1 and CDK6 in Du145 tumors from cells infected with MSCV-34a and LAPC4 tumors from cells infected with lenti-34a vectors.

Nature Medicine: doi:10.1038/nm.2284

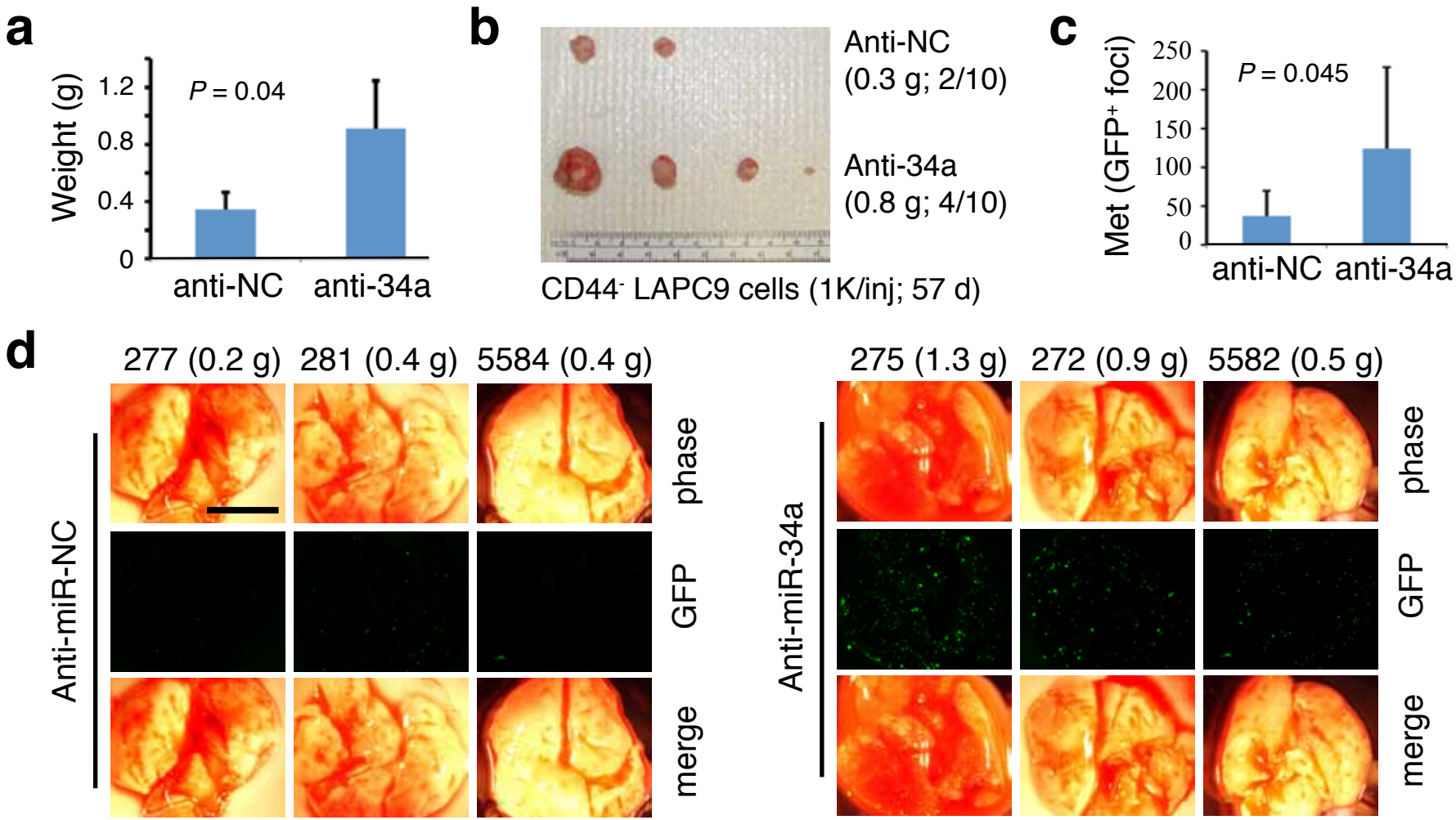

Supplementary Figure 7. Anti-miR-34a enhances LAPC9 tumor growth and lung metastasis.

(**a**) Anti-miR-34a promotes orthotopic LAPC9 tumor growth. This represents a repeat experiment to Fig. 1i. Shown are the mean weights of tumors derived from LAPC9-GFP cells transfected with anti-NC or anti-34a oligos and implanted in the DP of intact male NOD-SCID mice (sacrificed at 50 d). Tumor incidences for both groups were 4/7.

(**b**) Anti-34a promotes tumor growth of purified CD44$^-$ LAPC9 cells. Shown are the end-point tumors derived from CD44$^-$ LAPC9 cells transfected with anti-NC or anti-34a and s.c implanted in male NOD-SCID mice (euthanized at 60 d).

(**c**,**d**) Anti-miR-34a promotes orthotopic LAPC9 lung metastasis with data pooled from the two orthotopic tumor experiments (Fig. 1i and Supplementary Fig. 7a). Shown in d (and in Fig. 1j) are representative phase and GFP images of 4 lungs from each group (scale bar, 100 μm) and in c is the quantification of GFP$^+$ foci/lung.

Nature Medicine: doi:10.1038/nm.2284

Supplementary Figure 8. Competition experiments demonstrating clonality of PCa cell colonies and spheres.

(**a**) Clonal assays. Du145 cells were mixed with Du145-GFP cells at 1:1 ratio (50 cells each) and plated in 6-well plate. Images were taken on d 10 and shown are 3 representative fields.

(**b**,**c**) Clonogenic assays in methylcellulose (MC) or in Matrigel (MG). Du145 cells were mixed with DU145-GFP cells at 1:1 ratio and a total of 6,000 cells were plated for clonogenic assays in MC (b) or in MG (c). Photos were taken on d 5 after plating and shown are representative fields.

(**d**) Clonogenic assays in MC. Du145-RFP cells were mixed with Du145-GFP cells at 1:1 ratio and a total of 2,000 cells were plated in MC. Images were taken on d 4 and shown are two representative fields.

(**e**) Sphere-formation assays. Du145 cells were mixed with Du145-GFP cells at 1:1 ratio and a total of 2,000 cells were plated in ULA plates. Photos were taken on d 5 after plating and shown are a representative GFP^+ (left) and GFP^- (right) sphere.

Scale bars, 20 μm.

Nature Medicine: doi:10.1038/nm.2284

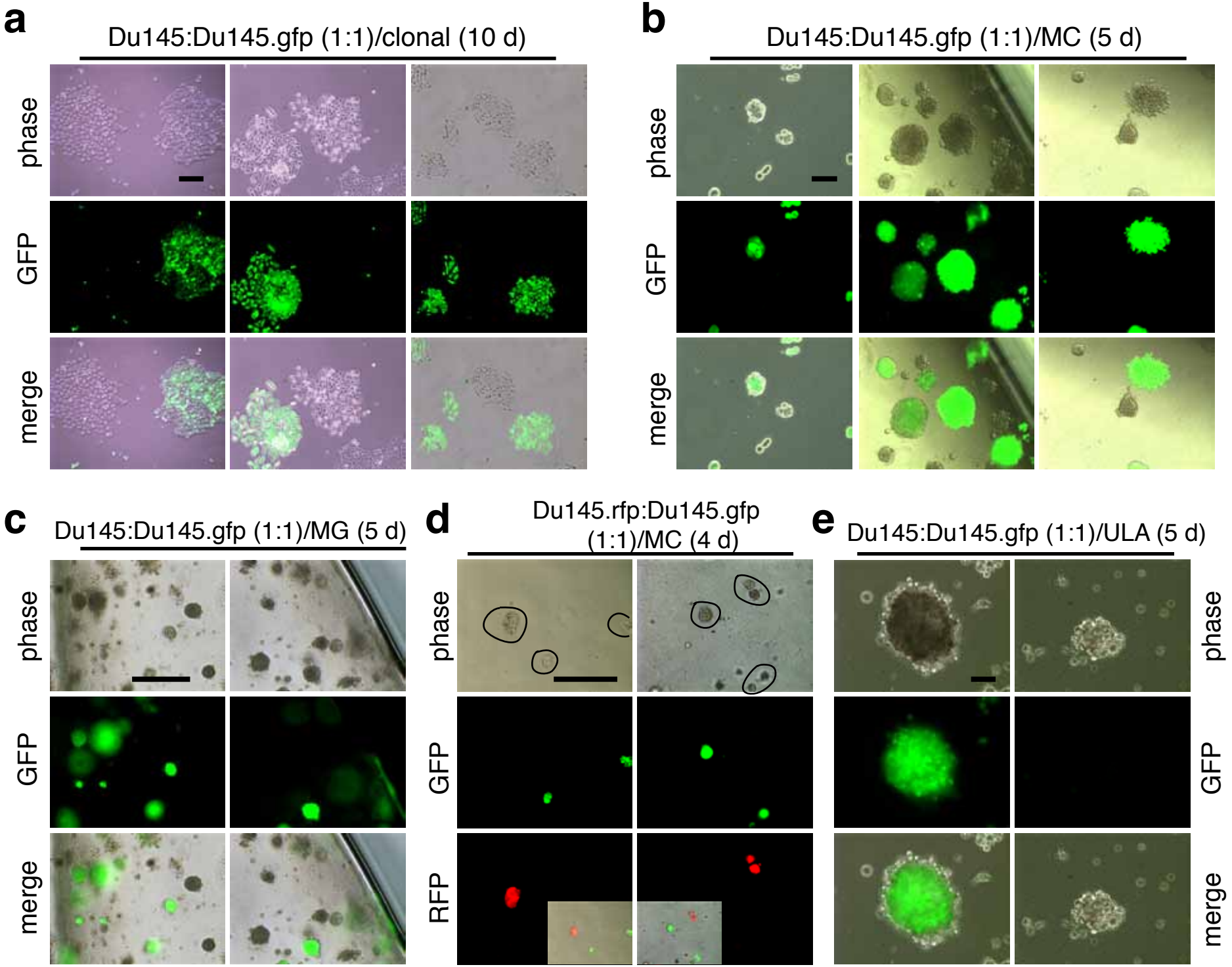

Nature Medicine: doi:10.1038/nm.2284

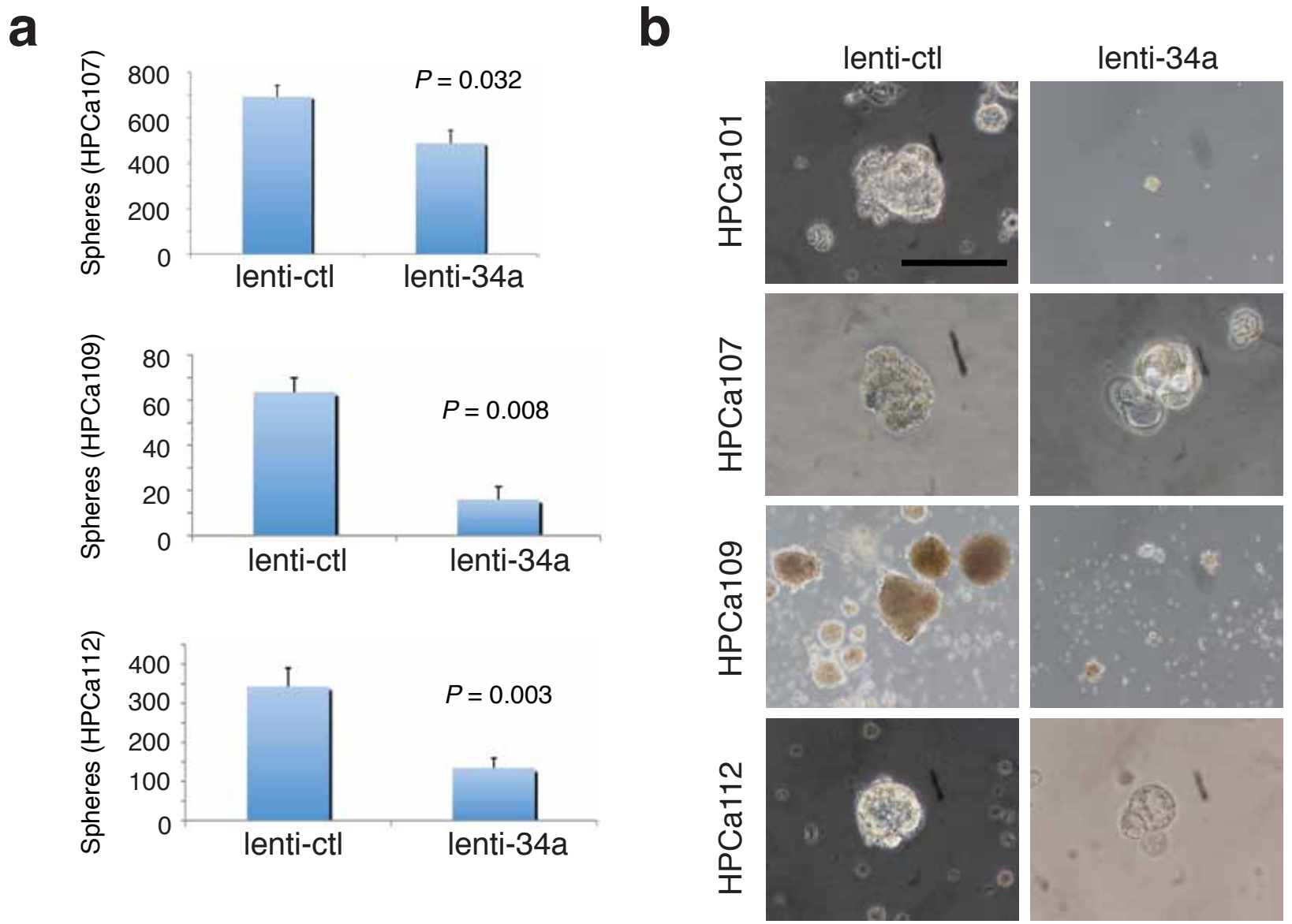

Supplementary Figure 9. miR-34a inhibits prostasphere formation in HPCa cells.
Presented in **a** are the numbers of spheres formed by HPCa cells freshly purified from the indicated patient primary tumors and infected with either lenti-ctl or lenti-34a vectors. Bars represent the mean ± s.d (n = 3–6). Shown in **b** are representative images of spheres formed by primary HPCa cells. Scale bar, 20 μm.

Nature Medicine: doi:10.1038/nm.2284

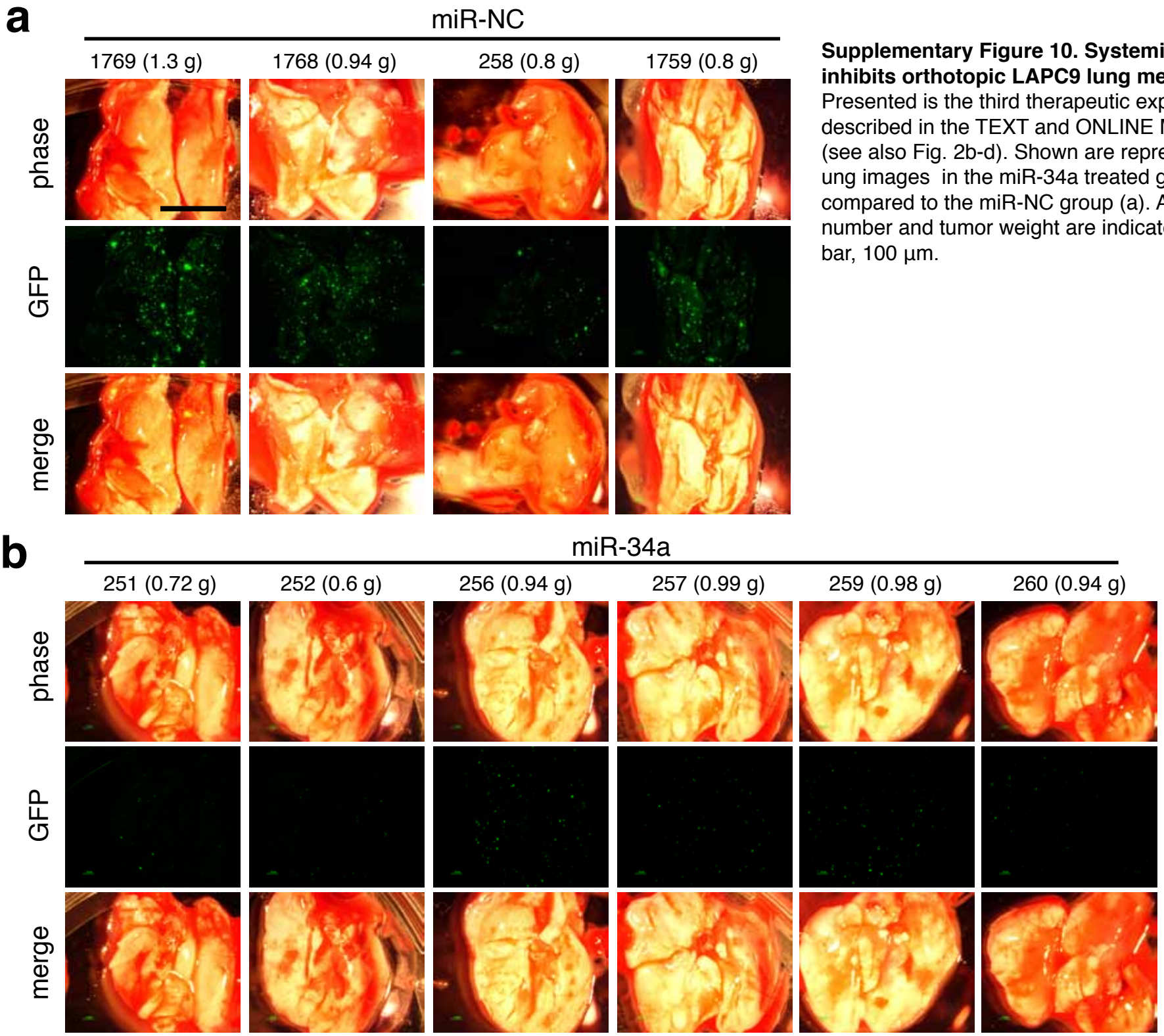

Supplementary Figure 10. Systemic miR-34a inhibits orthotopic LAPC9 lung metastasis. Presented is the third therapeutic experiment described in the TEXT and ONLINE METHODS (see also Fig. 2b-d). Shown are representative l ung images in the miR-34a treated group (b) compared to the miR-NC group (a). Animal tag number and tumor weight are indicated. Scale bar, 100 μm.

Nature Medicine: doi:10.1038/nm.2284

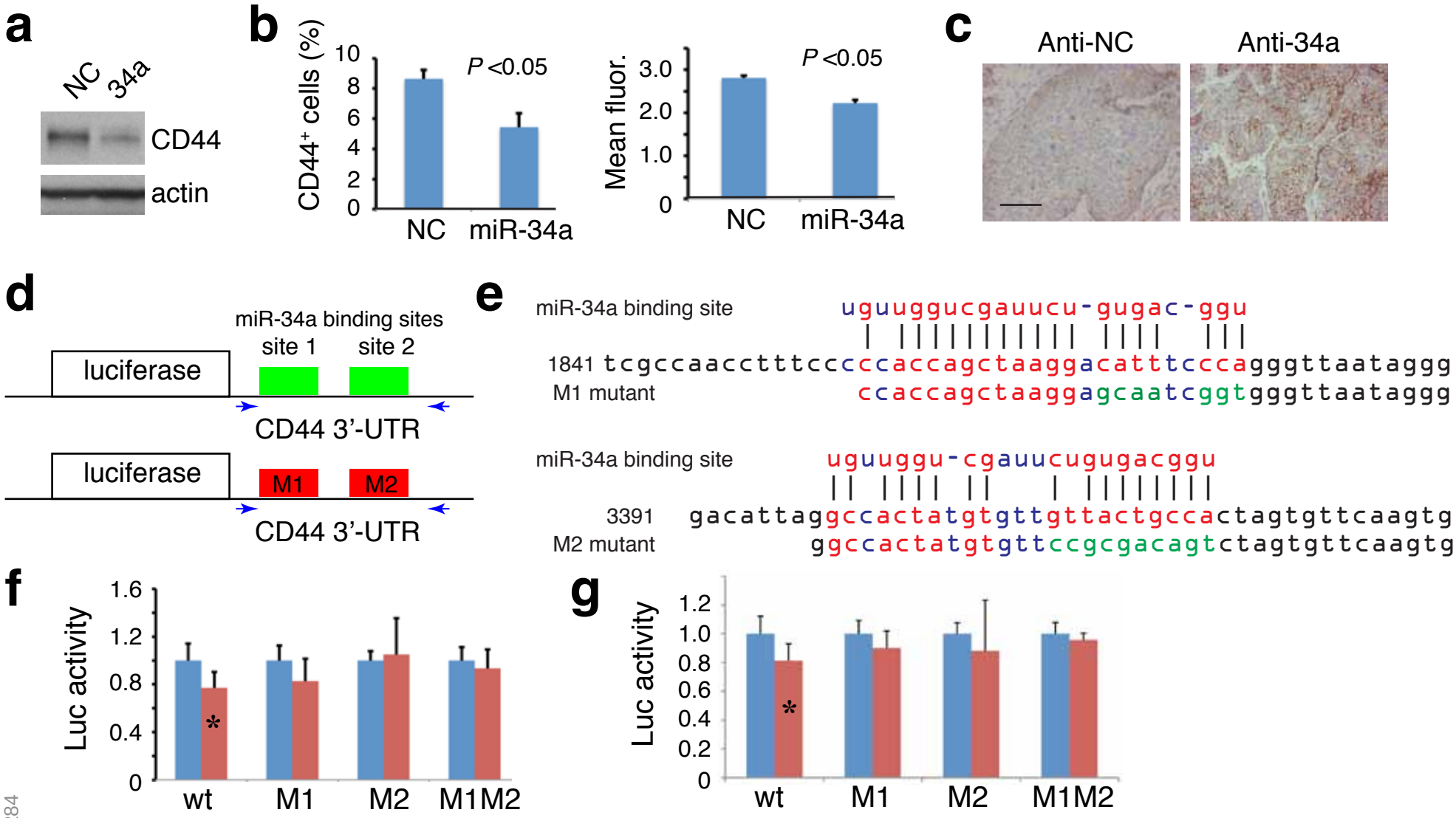

Supplementary Figure 11. miR-34a directly targets CD44.

(**a**) PC3 cells transfected with miR-NC or miR-34a oligos (33 nM, 48 h) were harvested and used in Western blotting of CD44 or β-actin.

(**b**) Purified LAPC9 cells were transfected with miR-NC or miR-34a oligos (33 nM; 72 h) and then used in flow cytometric analysis of CD44. Shown are CD44⁺ cells (%; $n = 3$) and the mean fluorescence intensity of CD44 expression.

(**c**) Two representative IHC images of CD44 staining in LAPC9 tumors derived from cells transfected with anti-34a or anti-NC. Scale bar, 10 μm.

(**d,e**) Schematic of the 2.55-kb wt CD44 3'-UTR containing the two miR-34a binding sites and the two mutants (i.e., M1 and M2) that were cloned downstream the luciferase cDNA in the 3'UTR/pMIR plasmid (d). Shown in e are the actual mutated sequences (in green).

(**f,g**) LNCaP (d) or LNCaP C4-2 (e) cells were co-transfected with wt or mutant luciferase construct together with NC (blue bars) or miR-34a (red bars) oligos. Each condition was run in 6 replicates and the experiment was repeated 2-3 times. The results were expressed as luciferase activity relative to the wt group after normalizing to the Renilla luciferase (internal control). Bars represent the mean ± SEM (*$P < 0.01$).

Nature Medicine: doi:10.1038/nm.2284

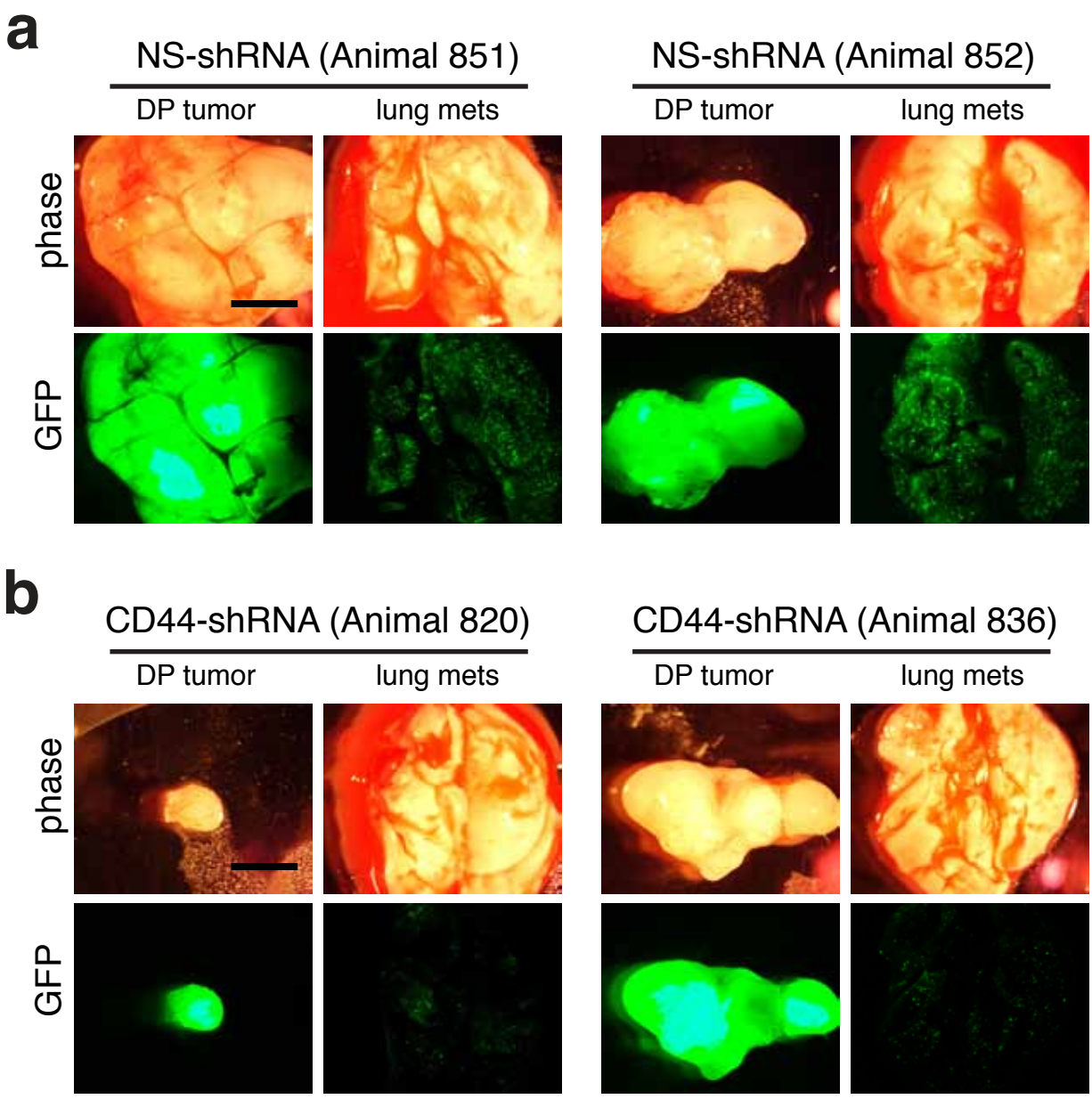

Supplementary Figure 12. CD44 knockdown inhibits LAPC4 lung metastasis. Purified LAPC4 cells infected with either non-silencing (NS) pGIPz control lentiviral vector or pGIPz-CD44shRNA (see Supplementary Fig. 1d) were implanted in the DP of male NOD-SCID mice (euthanized at 76 d). Shown are the images of DP tumors and the lungs from two representative animals in each group ($n = 7$). The CD44-shRNA animals (b) had both smaller DP tumors and less lung metastasis (GFP^+ foci) than in NS-shRNA animals. Scale bar, 100 μm.

Nature Medicine: doi:10.1038/nm.2284

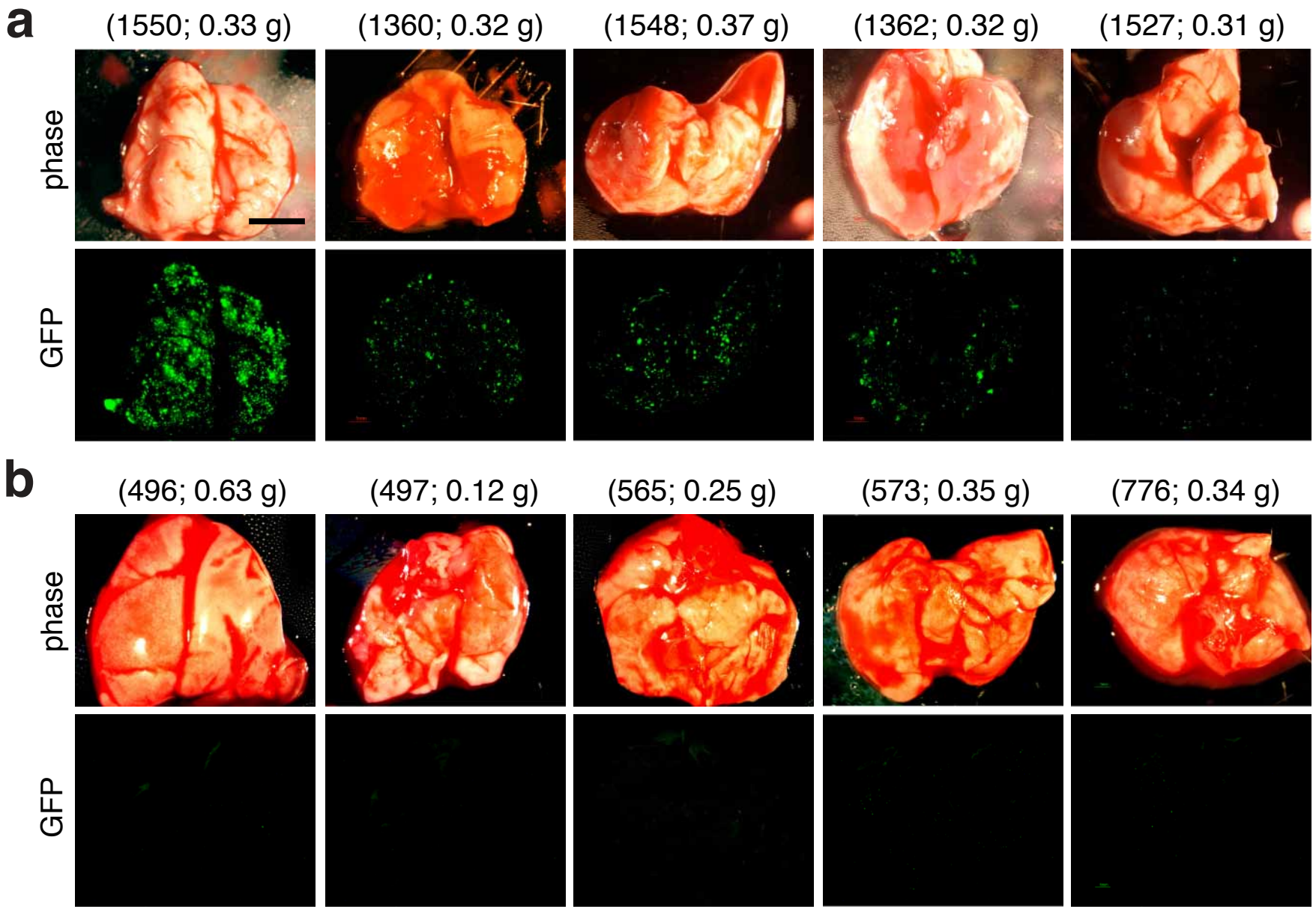

Supplementary Figure 13. CD44 knockdown inhibits PC3 cell lung metastasis.
Shown are phase and GFP images of five representative lungs in the animals bearing orthotopic PC3 tumors derived from cells infected with pGIPz control (**a**) or pGIPz-CD44shRNA (**b**) lentiviral vectors ($n = 8$ for each group; animals sacrificed at 40 d). Scale bar, 100 μm.

Nature Medicine: doi:10.1038/nm.2284

Supplementary Figure 14. Effects of CD44 knockdown or miR-34a overexpression on Du145 cells.

(**a**) Shown are the weights (above; mean ± s.d, $*P < 0.05$) and images (below; incidence, 5/5 for both groups) of subcutaneous tumors derived from Du145 cells infected with NS-shRNA or CD44-shRNA (MOI 20, 72 h; harvested at 56 d).

(**b**) Shown are the weights (above; mean ± s.d) and images (below) of orthotopic tumors derived from Du145 cells infected with NS-shRNA or CD44-shRNA (harvested at 41 d). Tumor incidence for the NS-shRNA and CD44-shRNA group was 7/7 and 5/8, respectively.

(**c**) Shown are the relative migratory abilities of purified $CD44^+$ and $CD44^-$ Du145 cells plated on the top of the Boyden chamber without Matrigel.

(**d**) Shown are two representative static images of $CD44^+$ (out of a total of 17 movies) and $CD44^-$ (out of a total of 14 movies) Du145 cells at the beginning of recording and at 7 h post wounding. In the movie images (scale bar, 20 μm) shown, the $CD44^+$ but not $CD44^-$ Du145 cells had closed the wound by 7 h.

(**e**) Shown are the relative invasive capacities of purified $CD44^+$ and $CD44^-$ Du145 cells plated on the top of the Boyden chamber with Matrigel.

(**f**) Shown are two representative static images of $CD44^+$ Du145 cells transfected with miR-NC (out of a total of 25 movies) or miR-34a oligos (out of a total of 29 movies) at the beginning of recording and at 5 h post wounding. Scale bar, 20 μm.

(**g**) Quantitative presentation of results in f.

Nature Medicine: doi:10.1038/nm.2284

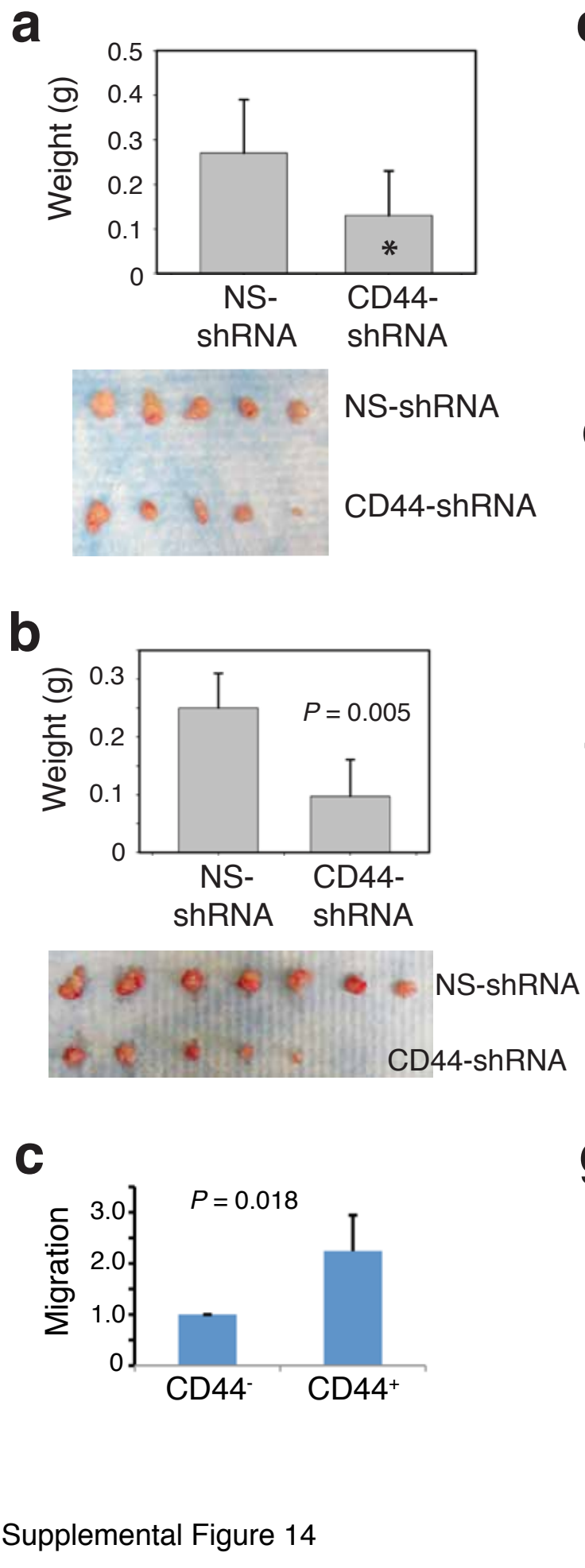

Supplemental Figure 14

Nature Medicine: doi:10.1038/nm.2284

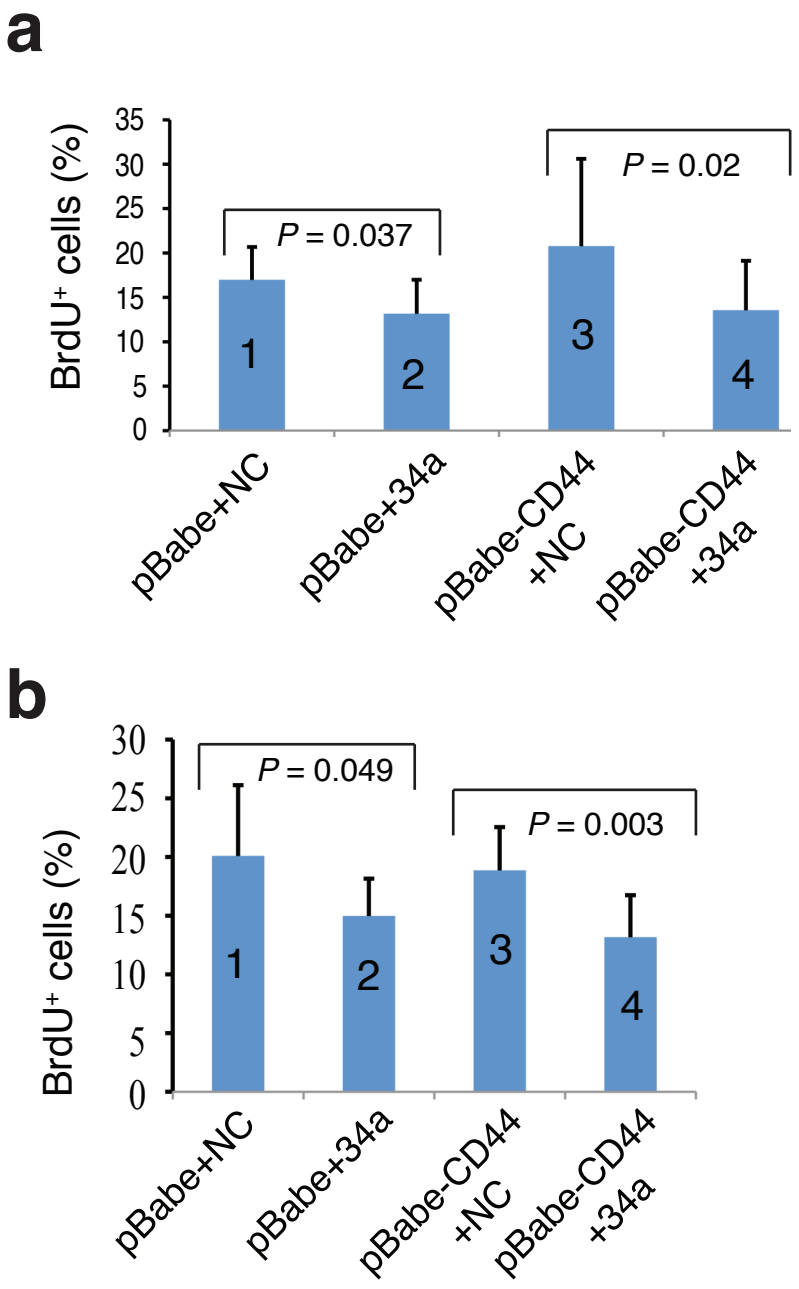

Supplementary Figure 15. CD44 overexpression does not relieve miR-34a-mediated inhibition of proliferation.

BrdU immunostaining in PPC-1 (**a**) or LNCaP (**b**) cells first infected with pBabe-CD44 (which encodes human CD44 cDNA that lacks the two miR-34a binding sites at the 3'-UTR) or its empty control vector (pBabe) and then (48 h later) transfected with miR-NC or miR-34a oligos oligos. Presented are the % BrdU$^+$ cells from counting a total of 400–500 cells in 2-3 experiments. In both cell types, miR-34a oligos reduced BrdU$^+$ percentages in cells infected with pBabe (conditions 1 and 2) or pBabe-CD44 (conditions 3 and 4). There were no differences between conditions 4 and 2 or between conditions 3 and 1 ($P > 0.1$).

Nature Medicine: doi:10.1038/nm.2284

Supplementary Table 1. Primary human prostate tumors (HPCa) used to purify CD44$^+$ and CD44$^-$ cells for qRT-PCR analysis

HPCa sample[a]	Age	Gleason	%CD44$^+$[b]	Purification[c]	Purity (%)[d]
HPCa60	54	8	8.7	MACS	CD44$^+$: ~50 CD44$^-$: N.A
HPCa62	59	7	2.4	MACS	CD44$^+$: ~50 CD44$^-$: 100
HPCa65	59	7	19.9	MACS	CD44$^+$: 67 CD44$^-$: 100
HPCa 66	58	6	15.0	FACS	CD44$^+$: N.A CD44$^-$: 94
HPCa72	58	7	10.2	MACS	CD44$^+$: 33 CD44$^-$: 100
HPCa74	59	7	16.2	MACS	CD44$^+$: 70 CD44$^-$: 100
HPCa76	64	7	0.02	MACS	CD44$^+$: ~10 CD44$^-$: 100
HPCa77	46	6	14.2	MACS	CD44$^+$: 45 CD44$^-$: 100
HPCa78	64	7	19.2	MACS	CD44$^+$: 45 CD44$^-$: 100
HPCa79	67	7	8.2	MACS	CD44$^+$: 15 CD44$^-$: 100
HPCa80	65	9	4.4	MACS	CD44$^+$: 13 CD44$^-$: 85
HPCa81	54	7	20.9	MACS	CD44$^+$: 64 CD44$^-$: 90
HPCa87*	57	9	N.D	MACS	CD44$^+$: 93 CD44$^-$: 100
HPCa89	55	9	24	MACS	CD44$^+$: 87 CD44$^-$: 90
HPCa91*	60	8	N.D	MACS	CD44$^+$: 95 CD44$^-$: 90
HPCa93	58	7	0.99	FACS	CD44$^+$: 87 CD44$^-$: 100
HPCa98	64	8	5.74	FACS	CD44$^+$: 79 CD44$^-$: 100
HPCa102	55	7	24.8	FACS	CD44$^+$: 99 CD44$^-$: 85

[a]Human primary tumors were obtained from the robotic (Da Vinci) surgery. The age and Gleason score of each tumor are indicated. *For HPCa87 and HPCa91, the first-generation xenograft tumors established in our lab were used in purifying CD44$^+$ and CD44$^-$ cells.

[b]The % of CD44$^+$ HPCa cells was determined by flow analysis prior to sorting. N.D, not determined.

[c]CD44$^+$ and CD44$^-$ cells were purified out using MACS (magnetic cell sorting) or FACS (fluorescence activated cell sorting). Four of the eighteen samples (shaded) were sorted using FACS as the MACS approach was more gentle on primary tumor cells.

[d]The purity of MACS-purified cells, determined by counting CD44$^+$ cells under a fluorescence microscope, was variable for both CD44$^+$ and CD44$^-$ cell populations. The purity of FACS-purified cells, determined by post-sort flow analysis, was ~80-99% for CD44$^+$ HPCa cells and 85-100% for CD44$^-$ cells. N.A, not available.

Nature Medicine: doi:10.1038/nm.2284

Supplementary Table 2. Correlation of CD44 levels with miR-34 manipulations in PCa cells

Tumor systems	Comments
LAPC9	– LAPC9 cells transfected with miR-34a oligos exhibit reduced CD44 protein expression levels and $CD44^+$ cells (**Supplementary Fig. 11b**). – LAPC9 tumors derived from cells transfected with anti-34a expressed higher levels of CD44 than tumors derived from the cells transfected with anti-NC (**Supplementary Fig. 11c**).
Du145	– Residual Du145 tumors from cells infected with MSCV-34a show reduced CD44 protein (**Fig. 4a**). – Du145 cells transfected with miR-34a oligos show time- and dose-dependent reduction in CD44 protein (**Fig. 4b**). – Du145 tumors derived from $CD44^-$ Du145 cells transfected with anti-34a expressed higher levels of CD44 mRNA than tumors derived from the same cells transfected with anti-NC (**Supplementary Fig. 4e**).
PC3	– Residual orthotopic PC3 tumors in animals treated with miR-34a display reduced CD44 protein (**Fig. 4a**). – PC3 cells transfected with miR-34a oligos show reduced CD44 protein (**Supplementary Fig. 11a**).
PPC-1	– PPC-1 cells transfected with miR-34a oligos show reduced CD44 protein (**Fig. 4b**).

Nature Medicine: doi:10.1038/nm.2284